Available online at www.sciencedirect.com
ScienceDirect
Catalysis Today 123 (2007) 285–292
CATALYSIS TODAY
www.elsevier.com/locate/cattod

Effect of engine-based thermal aging on surface morphology and performance of Lean NO_x Traps

Todd J. Toops [a,*], Bruce G. Bunting [a], Ke Nguyen [b], Ajit Gopinath [b]

[a] Oak Ridge National Laboratory, Fuels, Engines and Emissions Research Center, 2360 Cherahala Blvd., Knoxville, TN 37932-1563, United States
[b] University of Tennessee, Mechanical, Aerospace and Biomedical Engineering Department, 414 Dougherty Engineering Building, Knoxville, TN 37996-2210, United States

Available online 3 April 2007

Abstract

A small single-cylinder diesel engine is used to thermally age model (Pt + Rh/Ba/γ-Al_2O_3) lean NO_x traps (LNTs) under lean/rich cycling at target temperatures of 600 °C, 700 °C, and 800 °C. During an aging cycle, fuel is injected into the exhaust to achieve reproducible exotherms under lean and rich conditions with the average temperature approximating the target temperature. Aging is performed until the cycle-average NO_x conversion measured at 400 °C is approximately constant. Engine-based NO_x conversion decreased by 42% after 60 cycles at 600 °C, 36% after 76 cycles at 700 °C and 57% after 46 cycles at 800 °C. The catalyst samples were removed and characterized by XRD and using a microreactor that allowed controlled measurements of surface area, precious metal size, NO_x storage, and reaction rates. Three aging mechanisms responsible for the deactivation of LNTs have been identified: (i) loss of dispersion of the precious metals, (ii) phase transitions in the washcoat materials, and (iii) loss of surface area of the storage component and support. These three mechanisms are accelerated when the aging temperature exceeds 850 °C—the γ to δ transition temperature of Al_2O_3. Normalization of rates of NO reacted at 400 °C to total surface area demonstrates the biggest impact on performance stems from surface area losses rather than from precious metal sintering.

Keywords: Lean NO_x traps (LNT); Single-cylinder engine; Desulfation; Thermal aging; Rapid aging protocol

1. Introduction

Lean-burn technology is being slowly introduced into the automobile market in order to increase fuel efficiency and reduce emissions. A major challenge with lean-burn technology is the abatement of nitrogen oxides (NO_x), since unlike unburned hydrocarbons (UHC) and CO that react in an oxidizing environment, NO_x is most-efficiently reduced in a fuel-rich environment. Of the common de-NO_x technologies, the lean NO_x traps (LNT) is one of the leading candidates. LNTs are formulated with a storage component, usually alkali or alkaline earth metals, such as barium or potassium, and precious metals over a high surface area γ-Al_2O_3 support. During lean operation, NO_x is ''trapped'' in the storage component in the form of nitrates. For short periods the engine is operated slightly rich such that the stored nitrates are released as NO_x and subsequently reduced to N_2 by CO, H_2 and UHC over the precious metal sites [1–17]. Through successive cycles of lean and rich operating conditions, LNTs can achieve NO_x conversion efficiency greater than 90%.

Even though significant progress in improving LNT performance has been recently achieved, sulfur tolerance is a major hurdle that needs to be addressed before LNTs can be commercially viable. Like NO_x, sulfur is ''trapped'' on the storage component and can significantly diminish the storage capacity and LNT performance. Due to the increased thermodynamic stability of sulfates relative to nitrates, the temperature required to remove the sulfur is significantly higher. Thus, an LNT that typically operates between 200 °C and 500 °C must also be capable of maintaining activity after periodic thermal excursions to over 700 °C [17–23]. Although, operation at 700–800 °C is extreme and will lead to deactivation of most LNT catalyst systems, a primary concern of catalyst manufacturers is the more severe thermal excursions that can occur if precise engine control is not maintained. Inadvertent temperatures as high as 1000 °C are possible during

* Corresponding author. Tel.: +1 865 946 1207; fax: +1 865 946-1354.
E-mail address: toopstj@ornl.gov (T.J. Toops).

0920-5861/$ – see front matter © 2007 Elsevier B.V. All rights reserved.
doi:10.1016/j.cattod.2007.02.027

desulfation or other engine-controlled strategies during transient vehicle operation [24]. Additonally, the fuel or fuel-derived components in the exhaust gas during the rich excursions may be present on the LNT, and as the exhaust gases are switched to lean operating conditions in which the presence of oxygen is excessive, high-temperature excursions might be produced in the LNT. These high-temperature excursions are similar to fuel-cut exotherms experienced in three-way catalysts which can lead to overheating and thermal damage.

These high-temperature excursions during repeated regeneration and desulfurization are responsible for the thermal aging of the LNT which can lead to considerable deterioration in the performance of the LNT. The reduction of LNT performance is either caused by the loss of dispersion of Pt, the loss of surface area of the NO_x storage component and alumina support, or by phase transitions in the washcoat to a less capable storage medium such as $BaAl_2O_4$ [18,25,26]. Two of the key factors in the loss of Pt dispersion are temperature and the oxidative nature of the environment [27–34]; however, alternating from oxidizing to reducing conditions might retard this loss of Pt dispersion [34]. Furthermore, to accurately simulate engine operation, any rapid aging protocol for LNTs should include the switching of the exhaust stream between lean and rich conditions. In this study, LNTs are thermally aged by lean/rich cycling at elevated temperatures using a single-cylinder diesel engine and catalyst system. The effect of thermal aging on the surface morphology and the performance of LNTs are carried out using surface and chemical characterization techniques such as X-ray diffraction (XRD), N_2 physisorption, and H_2 chemisorption.

2. Experimental

A 500 cm^3 single-cylinder Hatz diesel engine (Model 1D50Z) was used for thermal aging of the LNTs. The engine and exhaust system shown schematically in Fig. 1, have been used for several diesel engine-based projects and is described in detail elsewhere [35–46]; only key features are described here. The engine produces a peak power of 10.5 hp at 3600 rpm and a peak torque of 21 ft-lbs at 2250 rpm. It is equipped with a special apparatus for injecting diesel fuel directly into the engine exhaust gas; thereby high-temperature rich excursions can be obtained for thermal aging. This injection apparatus consists of a positive displacement fuel pump, a small heater and an air atomization device. In addition to generating the high-temperature exotherms for aging catalysts, the fuel injection unit is used to regenerate the LNT. Ultra-low sulphur fuel is employed to reduce the effect of sulfur poisoning on the catalyst.

Two model LNT catalyst samples obtained from Engelhard, each 51 mm in diameter and 76 mm in length with a cell density of 300 cpi (cell per inch), are mounted in tandem in a catalyst holding assembly located approximately 2 m from the engine exhaust manifold. The model catalysts are comprised of Pt and Rh (14:1 ratio) and 30% BaO dispersed on a γ-Al_2O_3 support. The LNTs have an average washcoat loading of 225 g/L with a total precious metal loading of 5.3 g/L; the uncoated substrate density for the cordierite monolith is 570 g/L. The catalysts are wrapped with a ceramic fiber matt (Fiberfrax) before being inserted into the catalyst holder for insulation and protection from thermal expansion while also minimizing gas bypass. To

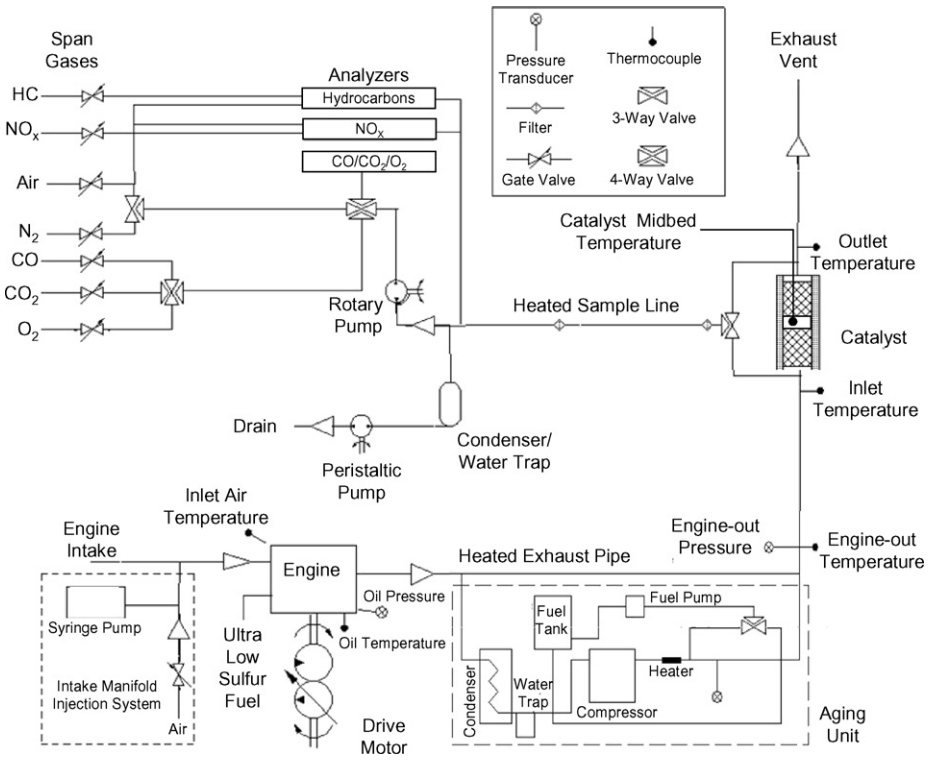

Fig. 1. Schematic of single-cylinder engine research apparatus.

monitor the LNT temperature, three type-K thermocouples are inserted at the inlet, the midbed and the exit of the catalyst assembly. In the present investigation, the aging temperature is indicated by the midbed temperature. All thermal aging experiments are performed at an engine speed of 1000 rpm with an average engine-out NO_x concentration of 1000 ppm and an exhaust gas temperature of 400 °C. This concentration is generally high, but is typical for this single-cylinder engine.

Prior to thermal aging, the LNTs are degreened for 4 h at an engine speed of 1000 rpm with the exhaust gas temperature maintained at 400 °C. During aging, the LNT is subject to target temperatures of 600 °C, 700 °C and 800 °C using a slow cycle comprising of 300 s lean and 120 s rich. The aging temperatures are achieved with a temperature controller and a supplemental fuel injection system. When running rich, the temperature controller cuts off the fuel injection when the LNT midbed temperature reaches the target aging temperature. The fuel injection is reactivated only when the temperature falls below the preset temperature. The fuel injection cycle is continued in this manner for the entire rich cycle in order to obtain the aging temperature profile. The slow cycle comprising of the lean and rich conditions is then repeated to obtain the required number of aging cycles. With this approach, the deactivation of the LNTs as a function of aging temperature and number of aging cycles can be obtained.

While aging the LNTs, NO_x conversion efficiency is periodically evaluated at 400 °C. This temperature is a tradeoff between the temperature for maximum NO_x conversion and the temperature required to keep the rich cycle on long enough to ensure adequate regeneration of the LNT. The cycle timer runs a fast cycle comprising of 20 s lean and 4 s rich for 5 min. During the rich phase, the temperature controller cuts off fuel injection when the LNT midbed temperature reaches the preset temperature of 400 °C and activates the fuel injection when the temperature falls below this temperature; this procedure is continued for the entire rich cycle. The NO_x conversion efficiency is obtained by averaging the NO_x concentration at the inlet and the oulet of the LNT assembly over a 5-min period. An analyzer bank capable of measuring simultaneously total hydrocarbons (THC), NO_x, and $CO/CO_2/O_2$ is employed for the measurements. All thermal aging and evaluation tests are performed at an engine speed of 1000 rpm and a gas-hourly space velocity (GHSV) of 60,000 h^{-1}.

The aged catalyst cores are sectioned for characterization of precious metal size, NO_x uptake, total surface area, and chemical phase of the NO_x storage medium and the support. Sections of fresh and aged LNT catalysts are characterized using an X-ray Diffractometer (PANalytical X'Pert Pro MPD Diffractometer) and a microreactor capable of performing NO_x storage and conversion measurements, plus pulsed chemisorption and BET. The microreactor is equipped with a Stanford Research System RGA100 mass spectrometer for effluent measurements during flow operation, and a Mensor 6100 DPT pressure transducer with 0.01 Torr precision during static operation. For smooth transition between lean and rich conditions a fast-switching, pneumatically controlled, four-way valve is used. To ensure equibaric operation, i.e., both exhaust ports on the four-way valve operate at the same pressure to minimize fluctuations, pressure transducers and a needle valve are employed in the vicinity of the four-way valve. A schematic of the microreactor is shown in Fig. 2.

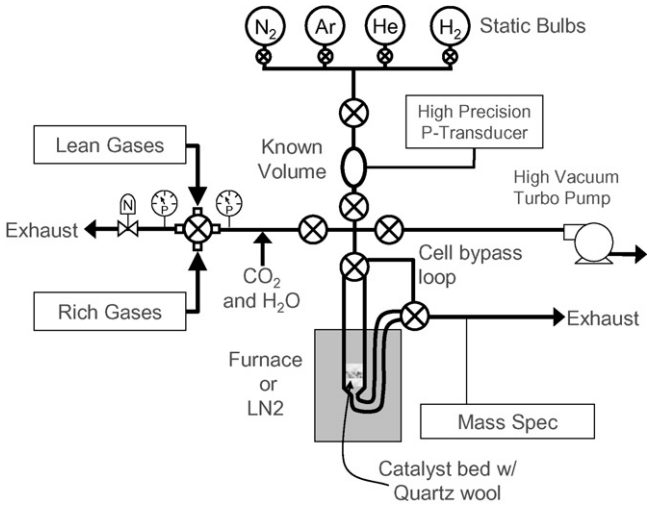

Fig. 2. Schematic of catalytic microreactor apparatus.

Three samples are obtained by cutting small wedges out of the engine-aged catalysts at three different locations: the inlet, the exit and the center sections. For XRD the LNT washcoat is scraped out of the channels to minimize cordierite interference. The microreactor samples, with the cordierite and washcoat intact, are ground into a powder less than 90 μm in diameter. A lower particle size limit is not used during sieving to maintain the catalyst loading in the powder form, i.e., each sample is continuously ground until the entire sample has passed through the sieve. Typically, 400 mg of total sample—washcoat, precious metals, and cordierite substrate—is used in each microreactor evaluation.

The performance of the LNT powder sample is evaluated at 400 °C in the microreactor using a simulated exhaust gas stream with a GHSV of 50,000–60,000 h^{-1}. The powder is exposed to a lean phase for 20s with a composition of 800 ppm NO, 10% O_2, 5% CO_2 and 4% H_2O, and a rich-phase of 3.4% CO, 1.1% H_2, 5% CO_2, and 4% H_2O for 4s. The catalyst powder is first pre-treated at 450 °C under a rich conditions and then cooled to 400 °C for evaluation. To determine the NO_x conversion, the system is allowed to operate until the NO_x profile of each lean–rich cycle is identical, i.e., cycle-to-cycle steady-state is achieved. NO_x storage is determined by reducing the catalyst under rich conditions at 450 °C, cooling to 400 °C, and then switching to the lean phase and monitoring NO_x uptake until the background level is observed in the effluent. Pulsed H_2 chemisorption is also performed in the microreactor using the four-way valve. With Ar flowing in one of the gas lines and a 1% H_2/Ar mixture in the second, a 2 s pulse of the H_2/Ar stream is introduced to the reactor every 60 s. This operation gives a consistent H_2 pulse, and once the Pt sites have been saturated with H_2, a characteristic peak is obtained in the mass spectrometer. The missing area in the initial peaks, compared to this saturated characteristic peak, allow

quantification of the Pt surface sites assuming a 1:1 ratio of atomic hydrogen to surface Pt. BET measurements are performed by evacuating the microreactor chamber to circa 10^{-6} Torr. Typical three-point BET protocol at −196 °C is performed using N_2.

3. Results

Characteristic LNT midbed temperature profiles at aging temperatures of 600 °C, 700 °C, and 800 °C are shown in Fig. 3. Due to the slow response of the temperature controller and the fuel injection system it is impossible to maintain a constant temperature during the rich phase of the aging cycle, and it is common for the fuel injection on/off sequence to occur at least three times during one aging cycle. During the rich phase of the aging cycle the LNT midbed temperature varies periodically with temperature excursions of 100–120 °C over the intended aging temperatures. The average temperature during the 5-min rich portion of each aging cycle is 620 °C, 690 °C, and 780 °C for target temperatures of 600 °C, 700 °C, and 800 °C, respectively. During the aging cycles, the NO_x conversion steadily decreases from 69% to as low as 30% as shown in Fig. 4. At each target temperature, an initially sharp decline in performance is observed during the first 10 aging cycles followed by a continued gradual decrease in performance.

To further understand the performance loss observed in the thermally aged LNTs, surface characterization and micro-reactor analysis are performed; the results are summarized in Table 1. The middle section of each catalyst wedge, both front and rear LNTs, is ground into a powder for the measurements as described in the previous section. The surface area of the entire washcoat and cordierite substrate are not severely affected after aging at 600 and 700 °C, whereas aging at 800 °C results in a 39–43% decrease in surface area from 28 m^2/g to 16–17 m^2/g. These total surface areas are low for these samples due to the inclusion of the cordierite; however, if cordierite's low surface area is accounted for, circa 1 m^2/g, and the washcoat loading is used, it is possible to determine the washcoat surface area as shown in the sixth column of Table 1. This estimate shows the same trend as the total surface area measurements with the washcoat surface area decreasing from 99 m^2/g to 57–60 m^2/g over the range of aging conditions.

Both H_2 chemisorption and XRD are employed to measure the extent of precious metal sintering and the results are

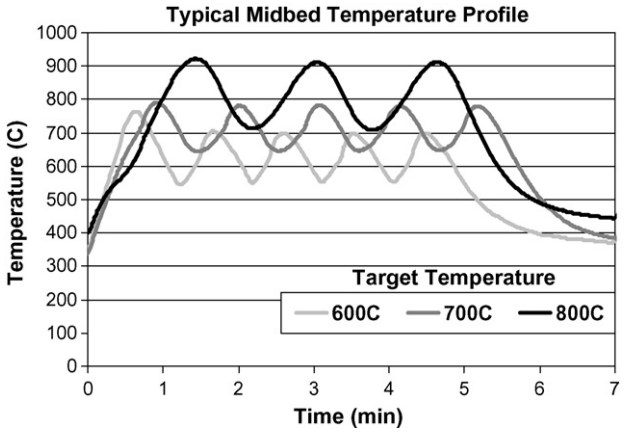

Fig. 3. Typical LNT midbed temperature profiles during engine-based thermal aging at target temperatures of 600 °C, 700 °C, and 800 °C.

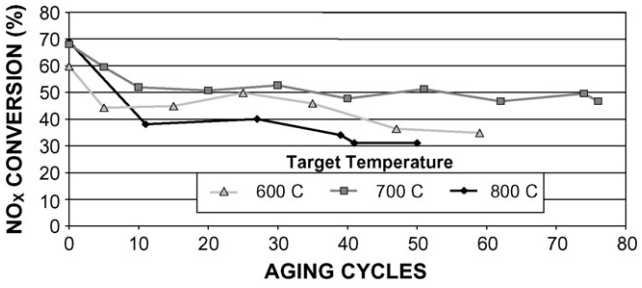

Fig. 4. Effect of aging temperature and number of aging cycles on-engine-based NO_x conversion.

tabulated in Table 1. The trends for both of these techniques are similar, and the absolute values show reasonable agreement. Similar to the surface area results, the precious metal shows an initial increase in particle size after aging at 600 °C (2.7–4.2 nm) and 700 °C (2.7–3.9 nm), but for the samples aged at 800 °C the extent of growth is more significant as the average particle size increases to 5.3–6.6 nm. The XRD patterns, where the sharpening of the Pt peak is evident, are depicted in Fig. 5. Another interesting feature of the XRD patterns is the change in the shape of the alumina peak at $2\theta = 68^\circ$ in the sample aged at 800 °C. The peak no longer has a Lorentzian shape and appears to have a high angle shoulder. This change in peak morphology is most likely due to the presence of a small fraction of the δ-Al_2O_3 phase which has three major peaks in this vicinity.

Table 1
Morphological properties and performance of fresh and aged LNTs

Target temperature (C)	Average temperature (C)	Aging cycles	Brick position	Total surface area (m^2/g)	Estimated washcoat surface area (m^2/g)	PM size-XRD (nm)	PM size-chemisorption (nm)	Storage capacity (μmol NO/g)	SS NO_x conversion (%)
Fresh	n/a	0	n/a	28	99	n/a	1.1	129	68
600	620	60	Front	25	89	3.6	3.0	138	64
600	620	60	Rear	26	92	4.2	2.7	135	72
700	690	76	Front	27	95	3.6	3.0	128	54
700	690	76	Rear	28	99	3.9	2.7	146	62
800	780	46	Front	16	57	6.2	5.3	82	43
800	780	46	Rear	17	60	6.6	6.1	73	44

Measurements performed in a microreactor or with XRD.

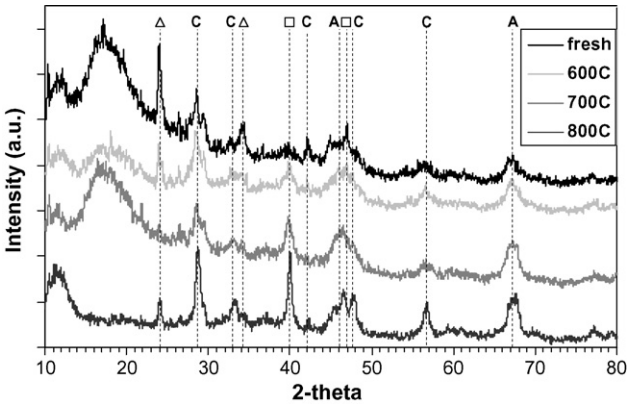

Fig. 5. XRD spectra of fresh LNT and LNTs aged at temperatures of 600 °C, 700 °C, and 800 °C. Legend: (△) Ba_2CO_3, (□) Pt, C: cordierite, A: γ-Al_2O_3.

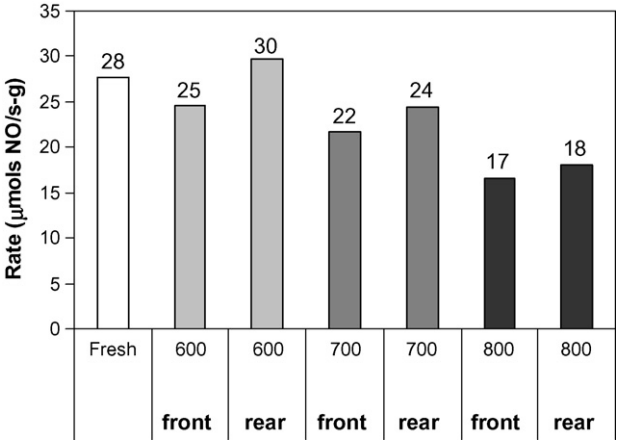

Fig. 6. Steady-state microreactor measurements of moles of NO reacted per gram of LNT catalyst averaged over one aging lean/rich cycle at 400 °C. The measurements were recorded after aging the samples at temperatures of 600 °C, 700 °C and 800 °C.

Around 860 °C, γ-Al_2O_3 is known to transition to the δ-phase, and since this catalyst sample is subject to temperatures as high as 920 °C (Fig. 3), it is not surprising to see the appearance of these peaks in the XRD pattern. $BaCO_3$ is the predominant Ba-phase observed in the XRD patterns, and although, care is taken to scrape only the washcoat off the substrate, the highly crystalline cordierite pattern is present in each sample due to small amounts of contamination. Although, cordierite inclusion was unintentional, it is interesting to observe that the cordierite peaks also seem to be sharpening at elevated aging temperatures. The Ba-phase also appears to be affected by aging, and this will be discussed further in the next section.

The saturation NO_x storage is measured at 400 °C for the fresh and aged catalysts, and the results are listed in Table 1. The storage capacity remains essentially constant for catalysts aged at either 600 or 700 °C, 128–146 μmol NO/g; however, for catalysts exposed to aging temperatures exceeding 800 °C the storage capacity decreases by 36–43% to 73–82 μmol NO/g.

The saturation storage capacity represents the maximum NO_x trapping capacity of the LNTs, but it only measures a portion of LNT function. The best method to evaluate full functionality in the microreactor system is by cycling between lean and rich conditions to mimic engine operation. This is performed using the same evaluation cycle employed in the engine-based evaluation—20 s lean and 4s rich at 400 °C. The average NO conversion for the entire cycle recorded at cycle-to-cycle steady-state is listed in Table 1. The initial conversion of 68% agrees well with the engine-based results, and even though the specific values may differ, due to the on-engine data being more prone to experimental variations, the aged catalysts show similar trends of decreasing performance—64–72% at 600 °C, 54–62% at 700 °C, and 43–44% at 800 °C. Although, conversion is often used to describe performance, it can be misleading since it is difficult to load the same amount of catalyst powder in the microreactor for each experiment. To circumvent this problem, the average rate of NO reacted is normalized to the catalyst mass; the results of this calculation are shown in Fig. 6. This clearly and accurately depicts a 35–40% decrease in activity as the LNT is aged above 800 °C. Also of interest in this figure is the consistently lower activity in the front LNT compared to the rear LNT. This trend is evidence of a probable higher exotherm experienced by the front LNT catalyst which is expected since the majority of the fuel is consumed in the front LNT, culminating in a higher temperature.

4. Discussion

The experiments described in this paper are the initial effort in establishing a rapid aging protocol for LNTs. This protocol is designed to elucidate procedures that quickly and accurately subject candidate catalysts to extreme conditions that typically occur during actual operation of LNTs. In establishing this protocol, it is important to determine the general rate of deactivation, the key mechanisms occurring and the relative importance of each. The operation of LNTs is complex in nature, so it is difficult to accurately reproduce the aging mechanisms without careful consideration. This engine-based approach captures the key dynamics that an on-board LNT would encounter—lean and rich conditions at typical desulfation temperatures and non-isothermal aging.

With the model catalysts used in this study, it is evident that a threshold temperature needed to be reached for there to be a significant decrease in surface area and increase in Pt size, and therefore a decrease in performance. This temperature threshold appears to be coincident with the transition of γ-Al_2O_3 to δ-Al_2O_3, but it is not immediately clear if the loss in surface area or the loss of exposed precious metal sites is most responsible for the decrease in performance. LNTs have four primary functions driving performance: the ability of precious metals to convert NO to NO_2, the ability of the Ba storage component to store NO_2 in the form of nitrates, the release of the nitrates during rich operation (precious metal catalyzed), and the ability of the precious metals to reduce the released NO_x to N_2 during short rich excursions. To further analyze the aged catalysts and to elucidate which characteristics are most responsible for performance loss, NO_x storage capacity is normalized on a

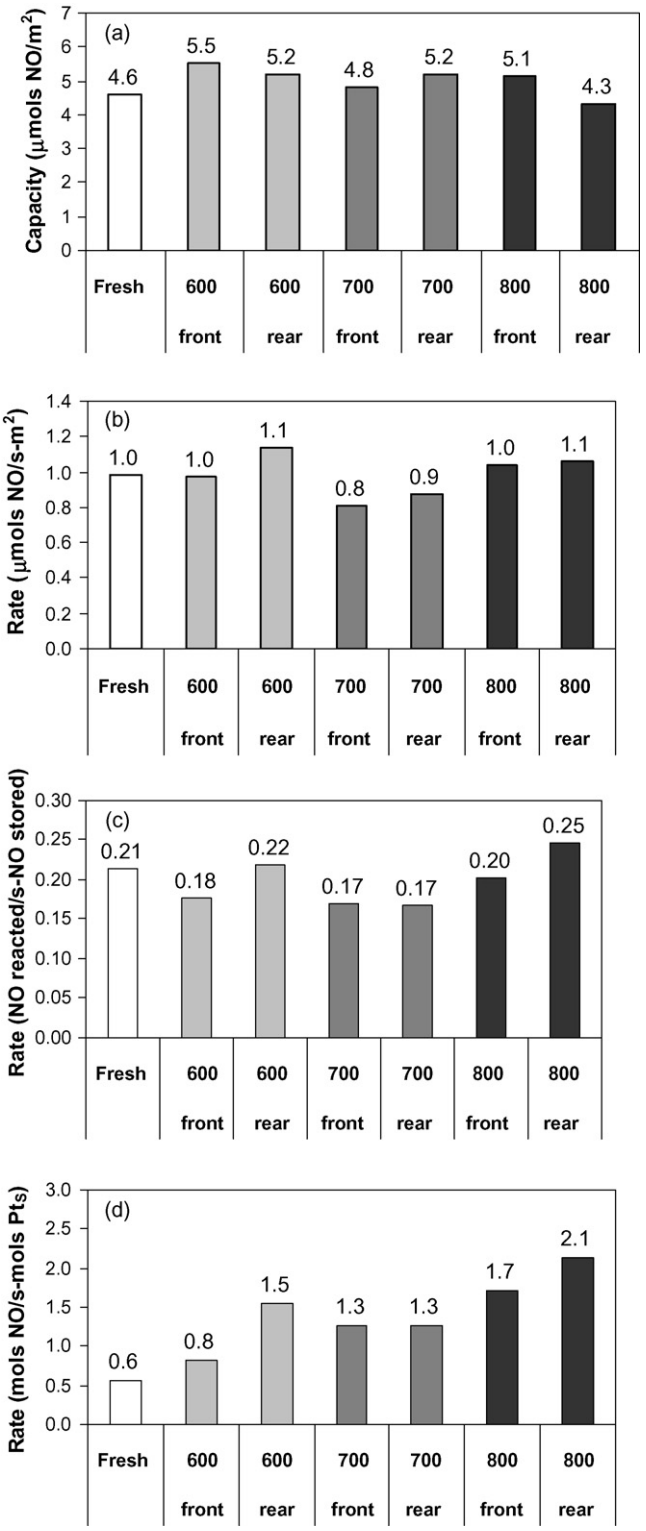

Fig. 7. Normalization of (a) storage capacity and (b) cycle-average steady-state NO reduction rate on an areal basis for the LNT catalysts thermally aged at 600, 700, and 800 °C. Rate of NO reduced normalized to (c) the measured NO_x storage capacity and (d) the precious metal surface sites (Pt_S) determined using H_2 chemisorption.

surface area basis. Fig. 7a shows that although the storage capacity decreases with aging temperature on a mass basis, when it is normalized to surface area the capacity is relatively constant for each of the catalysts—between 0.82 μmol NO/m^2 and 1.1 μmol NO/m^2.

At this point, it is important to discuss what phases seem to be most impacted by this surface area loss. The Pt surface area is definitely affected, but it has a small overall contribution to total surface area and can be neglected here. The other possible mechanisms leading to surface area losses are Ba agglomeration, alumina sintering, and a solid state reaction between the two phases leading to $BaAl_2O_4$. The XRD patterns suggest both Ba agglomeration and alumina transformation are occurring for the samples aged at a target temperature of 800 °C, but, as will be discussed in more detail below, it is not currently possible to determine the precise extent of either. However, it is clearly evident in these results that the storage capacity decrease is directly proportional to the surface area loss. Since these capacity measurements are meant to offer insight into Ba sites that are available at reaction conditions, this suggests that the Ba dispersion is directly correlated to total surface area.

A similar normalization can be extended with respect to reaction rate as well. The rates on a mass basis (Fig. 6) show a trend consistent with NO_x conversion reported in Table 1; however, when normalized to total surface area as shown in Fig. 7b, the rate is relatively constant after aging—between 4.3 μmol NO/(s m^2) and 5.5 μmol NO/(s m^2). This observation continues to suggest that the functionality of this catalyst is dependent on total surface area at 400 °C. A further comparison can be made by normalizing the rate of NO_x reduction with respect to NO_x storage capacity as shown in Fig. 7c. Not surprisingly, this also shows a relatively constant trend with respect to aging temperatures. Both of these results are very interesting, but it causes a dilemma since it is not possible to distinguish the effect of storage capacity versus total surface area. It is, however, possible to conclude that loss in total surface area and subsequently NO storage capacity are directly responsible for the decrease in performance of the LNT at 400 °C.

For an even more complete analysis, this approach should also be extended to precious metal surface area. Using the moles of precious metal surface sites (Pt_S), determined with pulse chemisorption, the molar rate of NO converted (mol/s) for the entire lean/rich cycle can be normalized to the precious metal exposed (mol NO/mol Pt_S/s). This approach is not a perfect measure of precious metal effectiveness, since at least four key rates are involved in the NO_x conversion; however, since it is not possible with our current setup to independently measure the rates of NO oxidation to NO_2, NO_2 storage, NO_2 release, and NO_2 reduction, this calculation will give a fair estimation of the precious metal effectiveness since the catalyst is necessary for the oxidation, release, and reduction steps. Fig. 7d depicts this normalized rate for the aged catalysts and actually suggests a significant increase in the effectiveness of the exposed precious metal. While this trend does not correlate to the overall NO_x performance, this increased effectiveness has been reported elsewhere with respect to NO oxidation [17,47–52]. It also

suggests that the key factor limiting LNT effectiveness after aging is the losses in storage capacity not the precious metal surface area. Since storage capacity is directly proportional to surface area it further suggests LNT functionality at 400 °C will depend on maintaining a high surface area and high barium dispersion, and although, the barium-phase can store significant NO_x in the bulk-phase, the access to these sites still depends on the exposed surface area of this storage component.

While it is possible to measure the Ba-phase particle size with XRD and determine the impact of Ba agglomeration, it is difficult to fully assess the Ba-phase characteristics in the XRD patterns. Clearly $BaCO_3$ is a predominant phase in the fresh sample and the samples that have been aged at 600 and 800 °C; however, at the target aging temperatures of 700 °C the $BaCO_3$ features are greatly diminished. It is known that LNTs can undergo phase transformation when exposed to ambient conditions [53], and the samples in this study were not rigorously controlled prior to the XRD characterization. Some catalysts used for XRD characterization had just recently been removed from the engine aging experiments, while others had been stored for up to 6 months before characterization. Consequently, it is difficult to draw specific conclusions from the Ba-phase analysis. $BaAl_2O_4$ is another expected phase that has been reported after high-temperature aging [34,53–58]; however, there is no indication of its existence in the present study. Our group has confirmed its formation in recent studies when aging temperatures exceed 900 °C [39,59,60].

5. Conclusions

Typical desulfation temperatures are between 700 °C and 800 °C for most LNTs, and it is expected that in-cylinder engine controls (fuel injection/timing) will be implemented to achieve the high temperatures. This study demonstrates the typical thermal profile during desulfation and shows when LNT catalyst temperatures exceed 800 °C three deactivation mechanisms are accelerated: (i) loss of dispersion of the precious metals, (ii) phase transitions of the adsorber material and support, and (iii) the loss of total surface area. Of these three mechanisms, the performance of this catalyst at 400 °C is closely correlated to the loss of total surface area and subsequently, the loss in NO_x storage capacity. To overcome loss of surface area and stabilize the alumina phase at high-temperatures, ceria has traditionally been incorporated into automotive three-way catalysts, and it is expected to have a role in commercial LNTs as well. Ceria-containing LNTs are currently being implemented in an incremental aging effort in our group that is designed to develop a more complete understanding of these thermal aging mechanisms [60], and in a related project, the fundamental impact ceria has on LNT chemistry and desulfation is also being studied [61].

Acknowledgments

This research was sponsored by the US Department of Energy under contract number DE-AC05-00OR22725 with the Oak Ridge National Laboratory with support and guidance of Steve Goguen, Dennis Smith and Kevin Stork. We would also like to acknowledge Joe Dettling, Stan Roth, C.Z. Wan, and Ken Voss of Engelhard, who were instrumental in providing catalysts, guidance, and fruitful discussions.

References

[1] L. Olsson, H. Person, E. Fridell, M. Skoglundh, B. Andersson, J. Phys. Chem. B 105 (2001) 6895.
[2] W. Boegner, M. Kramer, B. Krutsch, S. Pischinger, D. Voigtlander, G. Wenninger, F. Wirbeleit, M.S. Brogan, R.J. Brisley, D.E. Webster, Appl. Catal. B 7 (1995) 153.
[3] M.S. Brogan, R.J. Brisley, D.E. Webster, W. Boegner, M. Kramer, B. Krutsch, D. Voigtlander, SAE 952490, 1995.
[4] N. Miyoshi, S. Matsumoto, K. Katch, T. Tatanka, J. Harada, N. Takahara, SAE 950809, 1995.
[5] M.S. Brogan, R.J. Brisley, J.S. Moore, A.D. Clark, SAE 962045, 1996.
[6] G. Lutkemeyer, R. Weinowski, G. Lepperhoff, M.S. Brogan, R.J. Brisley, A.J.J. Wilkins, SAE 962046, 1996.
[7] M.S. Brogan, N.S. Will, M.V. Twigg, A.J.J. Wilkins, K. Jordan, R.J. Brisley, 6th Aachen Colloquium: Automobile and Engine Technology, Aachen, Germany, 1997.
[8] M.S. Brogan, A.D. Clark, R.J. Brisley, SAE TOPTEC Congress, September 1997.
[9] W. Strehlau, J. Leyrer, E.S.M. Lox, T. Keuzer, M. Hori, M. Hoffmann, SAE 962047, 1996.
[10] H. Mahzoul, J.F. Brilhac, P. Gilot, Appl. Catal. B 20 (1999) 47.
[11] M. Larsson, L. Andersson, O. Fast, M. Litorell, R. Makuel, SAE 1999-01-3503, 1999.
[12] Y.-W. Kim, J. Sun, I. Kolmanovsky, J. Koncsol, SAE 2003-01-1164, 2003.
[13] F. Laurent, C.J. Pope, H. Mahzoul, L. Delfosse, P. Gilot, Chem. Eng. Sci. 58 (2003) 1793.
[14] W.S. Epling, J.E. Parks, G.C. Campbell, A. Yezerets, N.W. Currier, L.E. Campbell, Catal. Today 96 (2004) 21.
[15] O.H. Bailey, D. Dou, G.W. Denison, SAE 972845, 1997.
[16] L. Lietti, P. Forzotti, I. Nova, E. Tronconi, Appl. Catal. 204 (2001) 175.
[17] W.S. Epling, L.E. Campbell, A. Yezerets, N.W. Currier, J.E. Parks II, Catal. Rev. 46 (2) (2004) 163.
[18] J.S. Hepburn, E. Thanasiu, D.A. Dobson, W.L. Watkins, SAE 962051, 1996.
[19] M. Guyon, F. Blejean, C. Bert, Ph.Le Faou, SAE 982607, 1998.
[20] S. Erkfeldt, M. Larsson, H. Hedblom, M. Skoglundh, SAE 1999-01-3504, 1999.
[21] S. Geckler, D. Tomazic, J. Orban, V. Scholz, R.A. Gorse, M.V. Whalen, O.H. Bailey, D. Mckinnon, J.C. Hoezler, SAE 2001-01-0510, 2001.
[22] D. Dou, O.H. Bailey, SAE 982594, 1998.
[23] E. Fridell, H. Persson, G. Westerberg, L. Olsson, M. Skoglundh, Catal. Lett. 66 (2004) 71.
[24] B. West, S. Huff, J.E. Parks, DOE Merit Review and Peer Evaluation Report, Advanced Combustion Engine Program, Argonne, IL, 2005.
[25] U. Goebel, J. Hoehne, E.S. Lox, W. Mueller, A. Okumara, W. Strehlau, SAE 1999-01-1285, 1999.
[26] N. Fekete, R. Kemmler, D. Voigtlaender, B. Krutsch, E. Zimmer, G. Wenniger, W. Strehaluu, J.A.A. Van Den Tillart, J. Leyner, E.S. Lox, W. Mueller, SAE 970746, 1997.
[27] F.M. Dautzenberg, H.B.M. Wolters, J. Catal. 51 (1978) 26.
[28] R.A. Hebermann, S.F. Adler, M.S. Goldstein, R.M. DeBaun, J. Phys. Chem. 65 (1961) 2189.
[29] T.R. Hughes, R.J. Houston, P.R. Seig, Ind. Engr. Chem. Proc. D. D. 1 (1962) 96.
[30] H.J. Matt, L. Moscou, Proc. Int. Congr. Catal. 3 (1965) 1277.
[31] G.A. Somorjai, in: H. Van Olphen, W. Parrish (Eds.), X-Ray and Electron Methods of Analysis, Plenum, New York, 1968 (Chapter. 6).
[32] P.A. Sermon, G.C. Bond, Catal. Rev. 8 (1973) 211.
[33] S.E. Wanke, J.A. Szymura, T.T. Yu, in: E.E. Peterson, A.T. Bell (Eds.), Proceedings of the. 3rd Int. Symp. Catal. Deact., Dekker, New York, 1986, p. 65.

[34] G. Graham, H.W. Jen, W. Chun, H. Sun, X. Pan, R. McCabe, Catal. Lett. 93 (2004) 129.
[35] B.G. Bunting, J.P. Szybist, T.J. Toops, K. Nguyen, S.J. Eaton, A.D. Youngquist, A. Gopinath, SAE 2006-32-0035.
[36] B.G. Bunting, K.L. More, S.A. Lewis, T.J. Toops, SAE 2005-01-1758.
[37] B.G. Bunting, K. Nguyen, SAE Vietnam Paper 007 International Conference on Automotive Technology for Vietnam, Hanoi, Vietnam, October 2005.
[38] S.J. Eaton, K. Nguyen, B.G. Bunting, SAE 2006-01-3422.
[39] H. Kim, K. Nguyen, B.G. Bunting, T.J. Toops, C. Yoon, 2007-01-0470.
[40] B.G. Bunting, J.P. Szybist, SAE 2007-01-0224.
[41] B.G. Bunting, SAE 2006-01-0872.
[42] J.T. Farrell, B.G. Bunting, SAE 2006-01-3275.
[43] J.P. Szybist, B.G. Bunting, SAE paper 2005-01-1758.
[44] S.A. Lewis, J.M. Storey, B.G. Bunting, J.P. Szybist, SAE paper 2005-01-3737.
[45] B.G. Bunting, Presented at SAE Homogeneous Charge Compression Ignition Symposium, Lund, Sweden, September, 2005.
[46] B.G. Bunting, C.B. Wildman, J.P. Szybist, S.A. Lewis, J.M Storey, Int. J. Engine Res., manuscript US/RR 72-12/22/05, in press.
[47] S.S. Mulla, N. Chen, L. Cumaranatunge, W.N. Delgass, W.S. Epling, F.H. Ribeiro, Catal. Today 114 (2006) 57.
[48] J.-H. Lee, H.H. Kung, Catal. Lett. 51 (1998) 1.
[49] E. Xue, K. Seshan, J.R.H. Ross, Appl. Catal. B 11 (1996) 65.
[50] S. Benard, L. Retailleau, F. Gaillard, P. Vernoux, A. Giroir-Fendler, Appl. Catal. B 55 (2005) 11.
[51] L. Olsson, E. Fridell, J. Catal. 210 (2002) 340.
[52] P. Denton, A. Giroir-Fendler, H. Praliaud, M. Primet, J. Catal. 189 (2000) 410.
[53] D.H. Kim, Y.H. Chin, J.H. Kwak, J. Szanyi, C.H.F. Peden, Catal. Lett. 105 (3/4) (2005) 259.
[54] T. Szailer, J.H. Kwak, D.H. Kim, J. Szanyi, C. Wang, C.H.F. Peden, Catal. Today 114 (2006) 86.
[55] C. Paze, G. Gubitosa, S.O. Giacone, G. Spoto, F. Xamena, A. Zecchina, Top. Catal. 30/31 (2004) 169.
[56] S. Elbouazzaoui, X. Courtois, P. Marecot, D. Duprez, Top. Catal. 30/31 (2004) 493.
[57] M. Eberhardt, R. Riedel, U. Gobel, J. Theis, E.S. Lox, Top. Catal. 30/31 (2004) 135.
[58] M. Casapu, J.D. Grunwaldt, M. Maciejewski, M. Wittrock, U. Gobel, A. Baiker, Appl. Catal. B 63 (2006) 232.
[59] A. Gopinath, M.S. Thesis, University of Tennessee, in preparation.
[60] N. Ottinger, M.S. Thesis, University of Tennessee, in preparation.
[61] Y.Y. Ji, T.J. Toops, M. Crocker, in preparation.